Modified fiber optic sensor for highly precise identification of mercuric ion (Hg^{2+}) concentrations in aqueous solution

Engineering Research Express

PAPER

Modified fiber optic sensor for highly precise identification of mercuric ion (Hg^{2+}) concentrations in aqueous solution

Hummad Habib Qazi[1,*], **Mohd Rashidi bin Salim**[1], **Abu Sahmah Bin Mohd Supa'at**[1], **Iftikhar Ahmed**[2,*], **Misbah Sehar Abbasi**[3], **Muhammad Mahmood Ali**[4], **Sevia Mahdaliza Idrus**[1], **Abu Bakar bin Mohammad**[1], **Muhammad Sultan Irshad**[5] and **Farhat Yasmeen**[6]

[1] School of Electrical Engineering, Faculty of Engineering, Universiti Teknologi Malaysia, 81310 UTM, Skudai, Malaysia
[2] Energy Research Centre, COMSATS University Islamabad, Lahore Campus, (54000), Lahore, Pakistan
[3] School of Energy and Power Engineering, Xi'an Jiaotong University, (XJTU), Xi'an (710049), People's Republic of China
[4] Optical Fiber Sensors Research Centre, Department of Electronics and Computer Engineering, University of Limerick, Limerick, V94 T9PX, Ireland
[5] School of Materials Sciences and Engineering, Hubei University, Wuchang, Wuhan, Hubei, People's Republic of China
[6] Department of Chemistry, University of Engineering & Technology Lahore (54000), Pakistan
[*] Authors to whom any correspondence should be addressed.

E-mail: hqhummad3@live.utm.my, mrashidi@utm.my, abus@utm.my, Iftikhar@live.fr, misbahsehar.ms@gmail.com, mahmood.ali@ul.i.e, sevia@utm.my, bakar@fke.utm.my, sultan.danish93@gmail.com and f.yasmeen@uet.edu.pk

RECEIVED
5 November 2020

REVISED
22 February 2021

ACCEPTED FOR PUBLICATION
26 February 2021

PUBLISHED
1 April 2021

Keywords: optical fiber, D-shaped cladding, rapid selective detection, mercuric ion

Abstract

A fiber optic sensor for monitoring mercuric (Hg^{2+}) ions in the aqueous sample have been developed based on modified cladding. To fabricate a D-shaped sensing zone onto the multimode optical fiber lengthwise polishing was utilized using a mechanical end and edge polishing system. The produced sensing region has dimensions of 10 mm $\times$ 125 μm $\times$ 62 μm ($l \times w \times h$). A 2 μm thin layer of Al_2O_3 nanoparticles sensitized with 4-(2-pyridylazo)-resorcinol was deposited onto the sensing element of multimode fiber optic sensor to make it sensitive and selective for Hg^{2+} ions. The analytical results demonstrate that the sensing device has a linear response for Hg^{2+} ions concentration over a range from 4 to 16 ppm along with a 4 ppm limit of detection in an aqueous sample at room temperature. The selectivity of the sensor is examined for the recognition of Hg^{2+} ions in presence of other cations such as zinc and/or lead ions up to 16 ppm in an aqueous solution. The main merits of this fabricated sensor are easy and safe installation, rapid response, enhanced linear response range, and better selectivity towards Hg^{2+} ions.

1. Introduction

Metals along with their corresponding ions are abundant. Man-made exploitations have reformed and impeded natural cycles and cause to liberate of the metal ions in aquatic and worldly systems. Certainly, heavy metals are important for human health as well as for other organisms.

In contrast, certain heavy metals and their ions are often extremely toxic or may cause significant health effects, with a very limited dosage of these metals or ions [1–4]. Therefore, it is crucial to measure the exact amount of mercury and other toxic elements in various earth's atmosphere including rocks, soils, air, water, plants, animals, and even humans. Conventionally, electrochemical analysis [5–7], mass spectrometry [8–10], atomic absorption spectrometry [11, 12], fluorometry [13–15], luminescence spectroscopic techniques [16–18] are applied to detect the analyte in the sample of concern. Indeed, there is a significant challenge that remains around the research community despite the tremendous analytic progress of metal ions detection, and efficient assessment [19–21]. Besides, the majority of analytical techniques irrespective of the mode and media of application, the evolving working conditions demand more sensitive, swift, rapid, and selective sensing devices [22, 23].

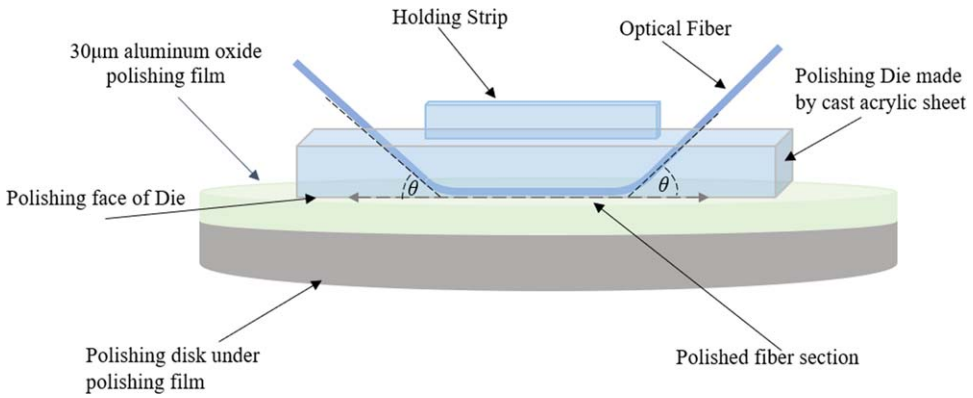

Figure 1. Schematic illustration of a polishing system.

During recent years, fiber optic sensors have gained escalating interest in the field of chemical, biochemical, and environmental science applications due to their potential to monitor analytes in real-time and *in situ* with minimum interruption to sample with higher sensitivity and desire selectivity. Moreover, the immune to electricity in the sensing system of fiber optic chemical sensors makes them more suitable to work in a harsh environment [24–26]. In principle, optical fibers are insensitive to the external environment and are designed to transfer data without affected by an external environment. Researchers working on optical fiber sensors have proposed various techniques to make an optical fiber sensitive to its surrounding environment [27–29]. Among them, one of the common techniques is to remove a certain portion of cladding so that the core is prone to the external environment. Consequently, alteration in the surrounding medium being sensed will cause a predictable change in light transmission characteristic of output light signals. Traditionally heat and pull technique [30] and chemical etching technique [31]. The sensing produced through the heat and pull technique is highly sensitive to the external environment. From a practical point of view, the huge loss of light signal and extremely fragile structure make these devices less suitable. On the other hand, unwanted residual cladding and poor surface roughness are major setbacks of the chemical etching technique. Alternatively, CO_2 laser or femtosecond laser machining can be used to produce a sensing zone onto the optical fibers [32–34]. In general, CO_2 laser machining can be used to strip the cladding of plastic optical fiber with desired dimensions. However, CO_2 laser machining cannot be used to produce a sensing zone onto the silica-based optical fibers. The femtosecond laser pulse is utilized to fabricate the D-shaped zone onto the silica-based optical fibers [32]. However, the lend of the sensing zone of the fabricated device was only 1 mm, which makes this reported device less suitable for sensing applications.

In this work, a modified cladding D-shaped fiber optic sensor is presented for the successful detection of mercuric ions concentration in an aqueous solution. A sensing zone was produced onto the multimode optical fiber using the side polishing technique. The main merits of the side polish technique are safe, fast, irrespective of the material of the optical fibers. This technique can be used to fabricate the sensing zone of all kind of optical fiber (e.g., plastic or silica-based optical fibers), the surface roughness of the sensing zone can also be control by choosing appropriately sized aluminum oxide polishing film and finally the dimension of the sensing zone also controllable. A thin film of aluminum oxide nanoparticles was employed as mesoporous transparent supports for 4-(2-Pyridylazo)-resorcinol (PAR), which acted as a sensing membrane. The performance of the sensor for different levels of mercuric ions concentration in the sample is analyzed. The turn-on method was applied to evaluate the response time of the sensing device. The performance of fiber optic chemical sensors (FOCS) has also been examined in presence of other potential metal ions (zinc and lead). Moreover, a comparative analysis of the present results along with previous studies from the literature indicated a measurable advancement in detection technology.

2. Fabrication of D-shaped fiber optic sensor

ULTRAPOL end & edge polishing system (model 3690.1) together with 30 μm layer of aluminum oxide polishing film were employed to fabricate D-shaped sensing region of 62.5/125 multi-mode fiber. The edge and ends of the waveguide were polished using a designed custom die. Since mechanical alteration was required to polish along the length of optical fiber. In order to generate a D-shaped sensing zone obtained by the lengthwise polishing of optical fiber, cast acrylic sheets were used for designing and fabricating the custom die.

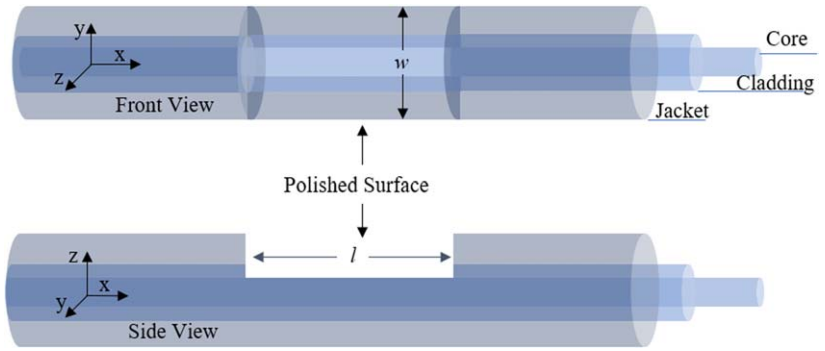

Figure 2. Conceptual illustration of D-shaped optical fiber sensor.

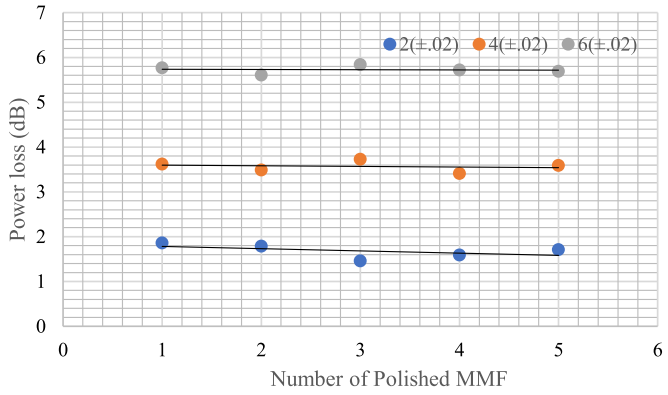

Figure 3. Power loss of each polished MMF (during and after the polishing process), three sets of single MMF (each set contains 5 optical fibers) were polished until transmission power loss was reached at 2 (±0.02), 4 (±0.02), and 6(±0.02) dB, respectively.

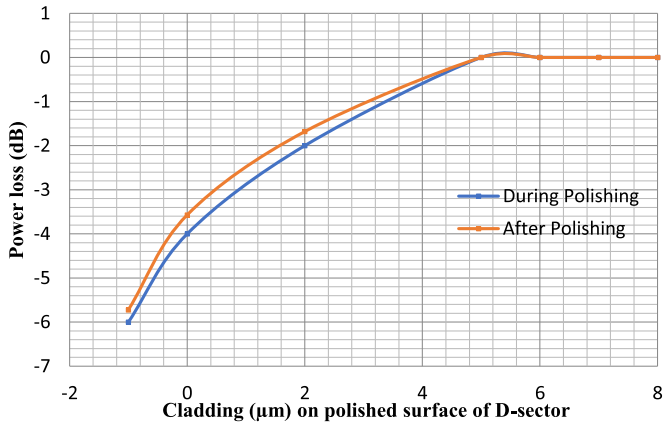

Figure 4. Average transmission power loss as a function of residual cladding on the polished surface of D-shaped MMF.

A schematic illustration of the polishing system with arrowed lines which shows the pathway of optical fiber in die is shown in figure 1. The angle between the tangential line of the polished end of dye and incoming light or light out ends is denoted as 'θ'. A light blue with a rectangular-shaped layer is a customized die with a dimension of 5.0 cm $\times$ 1.0 cm $\times$ 0.5 cm. It was made of a cast acrylic sheet and placed on the surface of aluminum oxide polishing film. Multimode optical fiber is threaded through both holes of the die and tightly fastened with cellophane tape to the upper surface of the die to avoid malposition during the entire polishing process.

It is essential to have a strong contact between the polishing film and the surface that is meant to be polished. Hence, a special holding strip was utilized in the center of the die structure. In order to have various angles concerning the horizontal plane between 20° and 45°, two tiny holes were drilled with the desired distance between them on the polished side. Both holes were drilled with a diameter of 1 mm each approximately. For the

Table 1. Power loss as a function of the residual cladding.

Operating wavelength (nm)	Input optical power (dBm)	Average Optical power loss (dB)		Length of the sensing zone	Residual cladding (μm)
		During polishing process	After polishing process		
1550 nm	12 dBm	2($\pm$.02) dB	1.68 dB	10 mm	$\approx 2\,\mu$m
1550 nm	12 dBm	4($\pm$.02) dB	3.58 dB	10 mm	$\approx 0\,\mu$m
1550 nm	12 dBm	6($\pm$.02) dB	5.72 dB	10 mm	$\approx -1\,\mu$m

sake of optimum performance during the polishing process, the variation angles we re-tested. The system used has the capability of polishing a waveguide surface up to 8 inches in length. It was observed that the length of the polishing surface with an angle lower than 20° is not capable to maintain stresses resulting from the rotatory motion of the polishing disk below and slowly causes the fiber to break. Needlessly, the length of the polishing surface rises beyond the aforementioned range. Similar results were observed for angles higher than 35°. Nevertheless, it was found that the angle at 30° was the most appropriate for the optimum polishing performance.

A conceptual illustration of D-shaped optical fiber is illustrated in figure 2. Where *l* and *w* are the length and width of the polished surface, respectively. Three sets of single multi-mode optical fibers were polished until the transmission power loss of each fiber set was at -2 ± 0.02, -4 ± 0.02, and -6 ± 0.02 dBm, respectively. The prepared set of multi-mode optical fibers contained 5 optical fibers. Each fiber from each set was polished separately and its power transmission was monitored in real-time and *in situ* throughout the entire polishing process. The power transmission loss of each polished fiber was recorded during and after the polishing process, as shown in figure 3. Readings after the polishing process were taken by unplugging the optical fiber from the polishing system. Table 1 summarizes the average transmission power loss as a function of residual cladding on the polished surface of D-sector multi-mode optical fibers during and after the polishing process, while figure 4 is a graphical presentation of table 1. Where 0 residual cladding means the fiber is polished at the edge of the core and minus sign means the core of the fiber is polished.

3. Chemicals

All reagents used were of analytical grade and employed as purchased regardless of more purification. Mercury (II) nitrate monohydrate ($Hg(NO_3)_2{\cdot}H_2O$), Zinc nitrate hexahydrate($Zn(NO_3)_2 \cdot 6H_2O$), Lead (II) nitrate ($Pb(NO_3)_2$), Potassium iodide(KI), Nitric acid (HNO_3), Sulfuric acid (H_2SO_4), Buffer Solution (pH 7) were purchased from Merck. While 4-(2-Pyridylazo)-resorcinol (PAR), Aluminum oxide nanoparticles (Al_2O_3) (50–60 nm particle size (TEM), 20wt. % in H_2O), and Hydroxypropyl cellulose were bought from Sigma-Aldrich. Doubly distilled water (DDW) was used throughout this work.

4. Preparation and deposition of sensing membrane on fiber optic sensor

Thin-film of Al_2O_3 nanoparticles was employed as mesoporous transparent supports for PAR. The sol-gel method was adopted for the synthesis of sensing membrane proposed by J.P. Hernández *et al* [35]. The dip-coating technique was employed to deposit the sensing membrane onto the sensing region of MMF. The preparation process was divided into three main phases. In the first phase, the paste was prepared, followed by the deposition of the prepared paste onto the sensing element of D-shaped multi-mode fiber and annealed. D-shaped MMF was treated in H_2SO_4 and indicator dye was immobilized onto the sensing membrane and hence fabrication of the fiber optic chemical sensor was completed.

The sol-gel method is as follows: A 15 ml of Al_2O_3 colloidal suspension and 0.35 g of hydroxypropyl cellulose were mixed slowly in a flask under vigorous stirring. This mixture was stirred for seven days at 65 ± 3 °C. Afterward, the resulting paste was let to be cool down and stored in the refrigerator until required for the further process. The reaction conditions and the morphology of the films were studied well and reported [35, 36].

For the sake of proper viscosity, at the time of deposition onto the D-shaped MMF, each 0.5 g prepared Al paste was diluted into 0.6 ml of absolute ethanol and dip coating technique was adopted. A robotic arm was used for the dipping process. The up/down velocity of the robotic arm was varied from 5 μm to 35 μm per second depending upon the viscosity of the paste. To ensure reproducibility a thin layer of 5 μm of paste was deposited onto the polished surface of D-shaped MMF. During the deposition process, microscopic measurements were continuously taken after every 2 to 3 cycles of coatings. Before taking each microscopic measurement, the

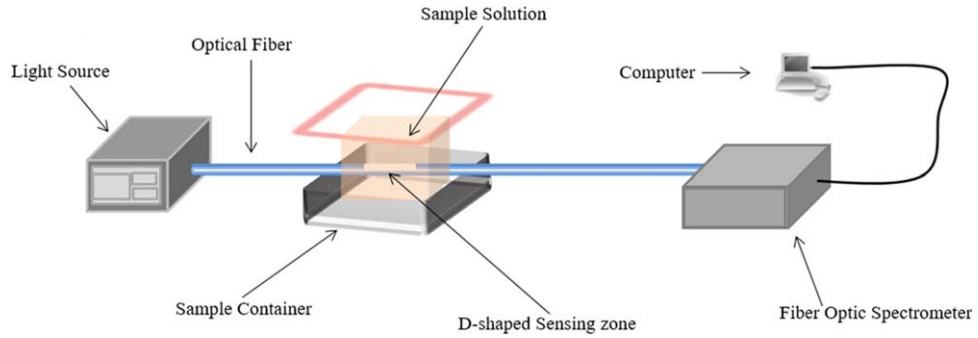

Figure 5. Schematic diagram of an experimental setup for D-shaped MMF Mercuric ion sensor.

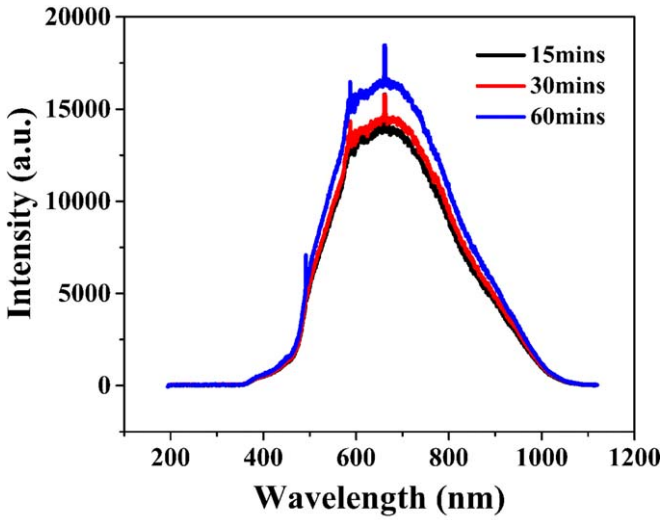

Figure 6. Intensity counts for the sensor after 15-, 30- and 45-minutes' time immersing in dye-ethanol solutions.

D-shaped MMF sensor could dry at room temperature for 5 min. As 4 μm this thin layer of paste is deposited onto the D-shaped MMF, it was annealed at 450 °C for 90 min for solidification purpose of the paste. After solidification at 450 °C, the thickness of the deposited film was found about 2 μm. The fiber was treated in H_2SO_4 at pH 1 for 20 min and let dry at 125 °C for 90 min, to enhance the stability of the sensing membrane. For the immobilization of the indicator dye onto the sensing membrane, the sensor was immersed in 0.3 mM PAR-ethanol for 15 to 45 min.

5. Experimental setup

A schematic diagram of the experimental setup for modified cladding D-shaped MMF sensor for Hg^{2+} ion in aqueous solution has been represented in figure 5. A white light source (DH-2000 Ocean Optics) with a wavelength range of 200–2500 nm was used as a light source. The light source was connected to one end fiber sensor, while the other end of the optical fiber was connected to the fiber optic spectrometer (HR4000 GC-UV-NIR, ocean optic) and the spectrometer was also connected to the computer for online monitoring purpose. The sample solutions were the aqueous solutions with various Hg^{2+} ion concentrations (2 ppm to 30 ppm). All sample solutions were prepared in the laboratory. The aqueous solutions with various concentrations of lead and zinc were also prepared in the laboratory to study the selectivity of the sensing device. Ocean-view (ocean optic) software version 1.4.1 was installed in the computer system for online monitoring.

6. Results and discussion

First, a non-sensitized modified cladding D-shaped MMF sensor was estimated by immersing into DDW, once the optical single was stable the optical intensity of blank water was measured, and, subsequently, 4 ppm of

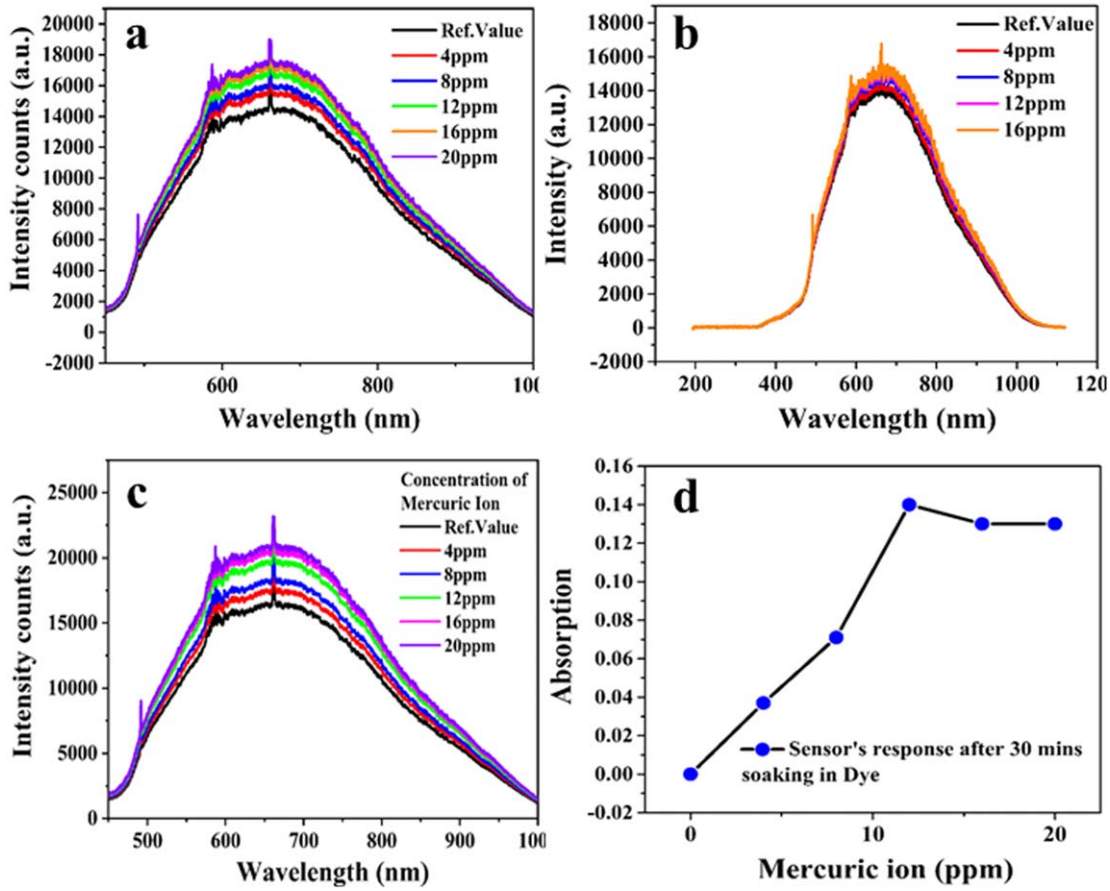

Figure 7. (a) Intensity counts as a function of the sensor's response with various concentrations of Mercuric ion in the sample (sensitization time 15 min). (b) Intensity counts as a function of the sensor's response with various concentrations of Mercuric ion in the sample (sensitization time 30 min). (c) Intensity counts as a function of the sensor's response with various concentrations of Mercuric ion in the sample (sensitization time 45 min). (d) The absorption as a function of sensor's response with various concentrations Mercuric ion solutions (sensitization time 30 min).

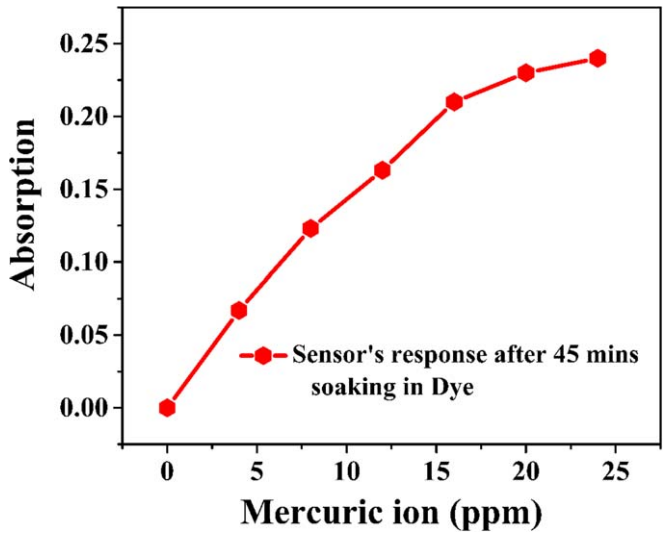

Figure 8. The absorption as a function of sensor's response with various concentrations Mercuric ion solutions (sensitization time 45 min).

Hg^{2+}ions were added. It was found that there was no change in the optical signal, for the concentration of Hg^{2+} ions up to 30 ppm in DDW. Therefore, it was anticipated that spectral change in optical single recorded with sensitized modified cladding D-shaped MMF sensor will not because of the change in RI of DDw due to Hg^{2+} ions exposure.

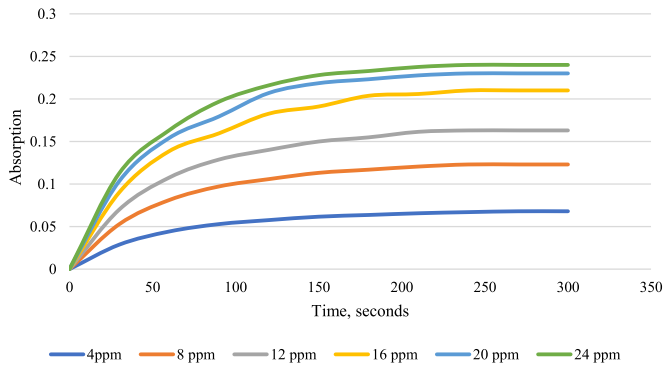

Figure 9. The absorption as a function of sensor's response time with various concentrations Mercuric ion solutions (sensitization time 45 min).

The immobilization time of indicator dye has a significant effect on the optical properties of the sensor as it has a direct influence on the response time and dynamic range of the sensor [37]. To investigate the optimal immersed time, the Al coated D-shaped multimode FOCSs were immersed in 0.3 mM PAR- ethanol solution for 15-, 30- and 45-minutes time intervals at room temperature. Then each FOCS was washed with DDw so that any excess of indicator dye on the sensing medium would be eliminated. Figure 6 presents the intensity counts for the sensor after 15, 30, and 45 min of immersing in dye-ethanol solutions. From the experiment, it was found that sensitization time of 30 and 45 min provide a more suitable spectral to examine the sensor's performance for Mercuric ion concentration in aqueous solutions. As shorter sensitization time (15 min) had poor spectral changes and shorter dynamic range.

The sensor exhibited remarkable spectral change when it was exposed to various concentrations of Hg^{2+} ions solutions pH 7. Figures 7(a)–(c) demonstrate intensity counts as a function of sensing devices' response when FOCSs were exposed to the various concentrations of Mercuric ion solutions after sensitization times of 15, 30, and 45 min, respectively. Depending upon the concentration of the analyte (Hg^{2+} ions) in the sample, light propagating inside the sensing membrane was partially absorbed, and the rest refracted back into the core [35]. The highest peak at 656 nm was observed, which was set up reference value to estimate the change in absorption as a function of FOCS response against the various concentration of Hg^{2+} ions in the sample. Figure 7(d) and figure 8 presents the absorption as a function of sensor response for the various concentration of Hg^{2+} ions at 656 nm. The concentration of Hg^{2+} ions was varied from 4 ppm to 20 ppm in aqueous solutions. To estimate the response time of the D-shaped multimode FOCSs were immersed in 0.3 mM PAR- ethanol solution for 45 min at room temperature absorption was taken as a function of sensor response for the various concentration of Hg^{2+} ions at 656 nm. The concentration of Hg^{2+} ions was varied from 4 ppm to 20 ppm in aqueous solutions. The response of the sensor was recorded after every 30 s for 5 min. Figure 9 presents absorption as a function of the sensor's response time when was expose to the various concentrations of Hg^{2+} ions solutions. The absorption was almost exponentially increased in the first minute of exposure to the Hg^{2+} ions, after work it is gradually stable. Finally, there is no change in an optical single after about 4 min of exposure to the Mercuric ion. Therefore, the sensor response time is 4 min.

Figures 8 and 9 demonstrate the variation in absorption versus various concentrations of Hg^{2+} ions in the sample solutions. It was found that an increase in Hg^{2+} ions concentration in sample solutions causes a linear increase in absorption and hence fabricated FOCS has a linear response for Mercuric ion concentration ranges from 4 ppm to 20 ppm in aqueous solutions. The gradient of 0.97 linear response was determined when it was sensitized for 45 min in 0.3 mM PAR-ethanol solution and it was 0.84 when it was sensitized for 30 min in the same solution. The selectivity of the sensor was also determined by adding $Zn(NO_3)_2 \cdot 6H_2O$) and ($Pb(NO_3)_2$) ions in the sample solutions. The absorption of the sensor was also monitored in presence of 16 ppm Hg^{2+} ions by adding $Zn(NO_3)_2 \cdot 6H_2O$) and/or ($Pb(NO_3)_2$) ions up to 16 ppm respectively, in the sample solution. It was found that the presence of $Zn(NO_3)_2 \cdot 6H_2O$) and/or ($Pb(NO_3)_2$) ions does not affect the output signal. It was concluded that the sensor has selectivity and sensitivity only towards Hg^{2+} ions in the samples of concern.

Besides the sensitivity and selectivity, reversibility of the analyte binding is another important characteristic of the sensing device. In fact, the reversibility of analyte binding determines whether the singing device is disposable (1time use) or it is a reusable device. To analyze the reusability of the reported sensor, first Al coated D-shaped multimode FOCS was immersed in 0.3 mM PAR- ethanol solution for 45 min at room temperature. Afterward, absorption is taken as a function of sensor response for 16 ppm concentration of Hg^{2+} ions at 656 nm. To extract Hg^{2+} ions from the sensing film, FOCS was immersed in 0.5 mM KI-solution for 5 before taking the sensor's response at the same operating wavelength. Figure 10 represents the successive reversibility

Table 2. Comparison of the presented FOCS with reported optical chemical sensor for the determination of Mercuric ions.

Analyte	Reagent or indicator	Sample	Linear response range	LOD	pH	Selectivity	Response time (mins)	Detection method	References
Hg^{2+}	Styryl (1,4,7,10-tetrathia-13-azacyclopentadecanyl) methyl coumarin (STAMC)	Aqueous solutions	0–28 μM	0.15 μM	7	Highly Selective	11 min	Fluorescence turn-on	[38]
Hg^{2+}	Acenaphtoquinoxaline	Aqueous solution	2–4 ppm	40 ppb	—	Selective	—	Fluorescence turn-on	[39]
Hg^{2+}	CdSe/ZnS QD	Aqueous solution	1–1000 nM	1 nM	7	Less selective	2 min	Fluorescence	[40]
Hg^{2+}	Ag-Fe bimetallic- 3-(Trimethoxysilyl) propyl methacrylate	River Water	10–50 nM	1.8 nM	5	Selective	—	Absorption	[41]
Hg^{2+}	Rh–3 S	Aqueous solution	2–80 μM	2 μM	7.3	Highly Selective	—	Absorption/ fluorescence	[42]
Hg^{2+}	Glucose capped silver nanoparticles (AgNPs)	Tap Water	2–200 ppb	5 ppb	—	Highly Selective	13 min	Absorption	[43]
Hg^{2+}	silver nanoparticle (CAgNP)	Aqueous solution	10–50 μM	10 μM	9	Selective	5 min	Absorption	[44]
Hg^{2+}	Chitosan (CS)/poly acrylic acid (PAA)	Aqueous solution	0–100 μM & 100–500 μM	0.0823 nm/μM & 0.017 nm/μM	5.41–10.51	Less selective in the presence of Ag^{+} and Fe^{3+}	40 min	Reflection	[45]
Hg^{2+}	Rhodamine 6 G	Aqueous solution	10–200 ppm	1 ppm	—	N/A	—	Absorption	[46]
Hg^{2+}	(PAH/PAA + AuNPs)n	Aqueous solution	1–20 ppb	0.7 ppb	7.6	Less Selective	—	Localized Surface Plasmon Resonances	[47]
Hg^{2+}	Gold nanoparticles (AuNPs)	Aqueous solution	1–30 μM	0.52 μM	3	Less selective	10 min	Localized Surface Plasmon Resonances	[48]
Hg^{2+}	polyelectrolyte (PE)- gold nanoparticles (AuNP)	Aqueous solution	2–5 ppm	—	—	N/A	10 min	Changes in the surrounding refractive index	[49]
Hg^{2+}	bis(2,2-bipyridyl-4,4-dicarboxylate) ruthenium (II) bistetrabutylammonium bis-thiocyanate	Aqueous solution	2 ppm to 6 ppm	2 ppm	7.0	Selective	5	Absorption	[35]
Hg^{2+}	PRA	Aqueous solution	4 ppm to 16 ppm	4 ppm	7.0	Selective	5	Absorption	This work

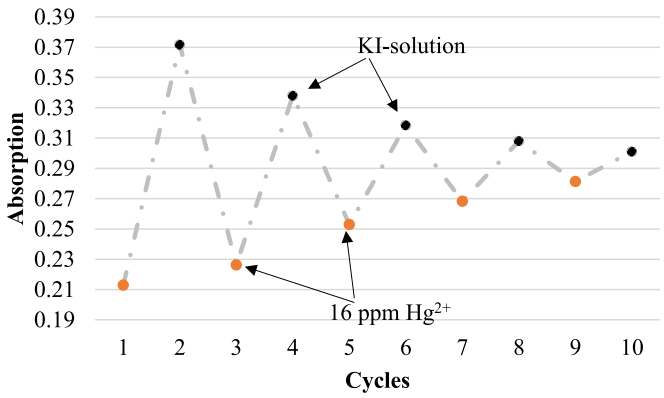

Figure 10. Reversibility of FOCS after exposing in KI-solution.

cycles by alternatively immersed FOCS in 16 ppm concentration of Hg^{2+} ions and 0. 5 mM KI-solution, while immersed in each solution was 5 min before monitoring the sensor's response. It is observed the sensitivity of the FOCS Hg^{2+} is gradually decreased after each reversible process.

The analytical results obtained from the research were also compared to the previously published analytical results in the literature. Table 2 represents prominent factors including (a) analyte of concern (b) reagents and indicators, (c) immobilization material (if any), (d) sample or solution in which analyte was analyzed, (e) linear response range, (f) limit of detection, (g) working pH value or range in which sensor's performance was optimized, (h) response time and (i) detection method, irrespective to sensing scheme employed to determine the Mercuric ions in the sample. It is clear from the cited literature that all these devices are struggling to achieve sensitivity and selectivity simultaneously, without compromising on response time. The most sensitive device was based on bis(2,2-bipyridyl-4,4-dicarboxylate) ruthenium(II) bistetrabutylammonium bis-thiocyanate [35]. But this reported device has a very short range of limit of detection i.e., 2 ppm to 6 ppm, only. It can also be seen in the table that most of the reported devices are also suffering from less selectivity. It is evident from the table that the sensor presented by this study has enhanced sensitivity towards Hg^{2+} ions in an aqueous solution. Moreover, the sensor described here has an enhanced dynamic range i.e., 4 ppm to 16 ppm which was about 170% enhanced to some of its competitors as shown in table 1.

7. Conclusion

In this work, a D-shaped MMF FOCS for monitoring the concentration of Hg^{2+} ions in an aqueous solution were introduced. To fabricate a D-shaped sensing zone onto the multimode optical fiber lengthwise polishing was utilized using a mechanical end and edge polishing system. A 2 μm thin layer of Al_2O_3 nanoparticles sensitized with 4-(2-pyridylazo)-resorcinol was deposited onto the sensing element of FOCS to make it sensitive and selective for Hg^{2+} ions. The analytical results demonstrate that the reported sensing device has a linear response for Hg^{2+} concentration over a range from 4 ppm to 16 ppm along with a 4ppm limit of detection in aqueous solutions at room temperature. In addition, this linear response range is about 170% enhanced compared to some of its competitors. Furthermore, the selectivity of the sensor has also been examined for the determination of Hg^{2+} ions in presence of other cations such as $Zn(NO_3)_2 \cdot 6H_2O$) and/or ($Pb(NO_3)_2$) ions up to 16 ppm in an aqueous solution sample. The main merits of this reported sensor are easy and safe fabrication, rapid response, enhanced linear response range, and better selectivity towards Hg^{2+} ions.

Acknowledgments

The authors are grateful to the officials at Research Management Center (RMC), Universiti Teknologi Malaysia for providing funds and resources to accomplish this research works well in time.

Data availability statement

The data that support the findings of this study are available upon reasonable request from the authors.

Declaration of competing interest

The authors declare that they have no known competing financial interests or personal relationships that could have appeared to influence the work reported in this paper.

Author Contributions

All authors significantly contributed to the manuscript.

ORCID iDs

Iftikhar Ahmed https://orcid.org/0000-0003-3523-300X
Muhammad Sultan Irshad https://orcid.org/0000-0002-2242-9874

References

[1] Wang R, Li H and Sun H 2019 Bismuth: environmental pollution and health effects *Encyclopedia of Environmental Health* p 415
[2] Mishra S *et al* 2019 Heavy metal contamination: an alarming threat to environment and human health in*Environmental Biotechnology: For Sustainable Future.* (Berlin: Springer) pp 103–25
[3] Madhav S *et al* 2020 Water pollutants: sources and impact on the environment and human health in*Sensors in Water Pollutants Monitoring: Role of Material.* (Berlin: Springer) pp 43–62
[4] Adimalla N 2020 Heavy metals pollution assessment and its associated human health risk evaluation of urban soils from Indian cities: a review *Environ. Geochem. Health* **42** 173–90
[5] Vimala A and Vedhi C 2019 Electrochemical sensors for heavy metals detection in gracilaria corticata using multiwalled carbon nanotubes modified glassy carbon electrode *J. Anal. Chem.* **74** 276–85
[6] Dai X, Wu S and Li S 2018 Progress on electrochemical sensors for the determination of heavy metal ions from contaminated water *Journal of the Chinese Advanced Materials Society* **6** 91–111
[7] Tang W *et al* 2018 Internal calibration potentiometric aptasensors for simultaneous detection of Hg2+, Cd2+, and As3+ based on a screen-printed carbon electrodes array *Anal. Chem.* **90** 8337–44
[8] Chen X *et al* 2013 Rapid speciation analysis of mercury in seawater and marine fish by cation exchange chromatography hyphenated with inductively coupled plasma mass spectrometry *J. Chromatogr. A* **1314** 86–93
[9] Kaur S *et al* 2019 Environmental copper sensor based on polyethylenimine-functionalized nanoporous anodic alumina interferometers *Anal. Chem.* **91** 5011–20
[10] Ding Y *et al* 2016 Nanomaterial-based optical sensors for mercury ions *TrAC, Trends Anal. Chem.* **82** 175–90
[11] Chen Y *et al* 2019 A carbon-supported BiSn nanoparticles based novel sensor for sensitive electrochemical determination of Cd (II) ions *Talanta* **202** 27–33
[12] Devi P *et al* 2019 Recent advances in carbon quantum dot-based sensing of heavy metals in water *TrAC, Trends Anal. Chem.* (https://doi.org/10.1016/j.trac.2019.03.003)
[13] Wang L *et al* 2019 Recyclable DNA-Derived polymeric sensor: ultrasensitive detection of Hg (II) ions modulated by morphological changes *ACS Appl. Mater. Interfaces* **11** 40575–84
[14] Shan Y *et al* 2019 On-site quantitative Hg2+ measurements based on selective and sensitive fluorescence biosensor and miniaturized smartphone fluorescence microscope *Biosens. Bioelectron.* **132** 238–47
[15] Lal S *et al* 2020 Curcumin based supramolecular ensemble for optical detection of Cu2+ and Hg2+ ions *J. Mol. Struct.* 128091
[16] Mahmoud W E, Yaghmour S and Al-Amri A M 2013 Enhancement of CdSe quantum dots luminescence by calcium ions *J. Lumin.* **134** 429–31
[17] Al-Ghamdi H S and Mahmoud W E 2014 Synthesis of self-assembly plasmonic silver nanoparticles with tunable luminescence color *J. Lumin.* **145** 880–3
[18] Al-Bluwi S A and Shirbeeny W 2020 The luminescence characteristics of multicolors-tunable Zn1-xErxSe QDs prepared via microwave irradiation technique for light emitting diode applications *Optik* **223** 165644
[19] Ferrari A G-M *et al* 2020 Recent advances in portable heavy metal electrochemical sensing platforms *Environmental Science: Water Research & Technology* **6** 2676–90
[20] Chauhan S and Upadhyay L S B 2020 Biosensor: a boon for heavy metals detection in natural water reservoirs at higher altitudes in*Microbiological Advancements for Higher Altitude Agro-Ecosystems & Sustainability.* (Berlin: Springer) pp 393–410
[21] Qazi H H 2016 D-shape optical fiber chemical sensor for multi parameters monitoring in*Faculty of Electrical Engineering* (Johor Bahru, Johor, Malaysia: Universiti Teknologi Malaysia)
[22] Irshad M S, Arshad N and Wang X 2020 Nanoenabled photothermal materials for clean water production *Glob. Challenges* **2000055** 20000–055
[23] Çaylak O *et al* 2019 Use of an aminated Amberlite XAD-4 column coupled to flow injection cold vapour generation atomic absorption spectrometry for mercury speciation in water and fish tissue samples *Food Chem.* **274** 487–93
[24] Gupta B D and Kant R 2018 Recent advances in surface plasmon resonance based fiber optic chemical and biosensors utilizing bulk and nanostructures *Opt. Laser Technol.* **101** 144–61
[25] Muginova S V *et al* 2017 Applications of ionic liquids for the development of optical chemical sensors and biosensors *Anal. Sci.* **33** 261–74
[26] Compagnone D *et al* 2017 Chemical sensors and biosensors in Italy: a review of the 2015 literature *Sensors* **17** 868
[27] Wang X-D and Wolfbeis O S 2020 Fiber-optic chemical sensors and biosensors (2015–2019) *Anal. Chem.* **92** 397–430
[28] Arshad N, Ahmed I, Irshad M S, Li H R, Wang X, Ahmad S, Sharaf M, Firdausi M, Zaindin M and Atif M 2020 Super hydrophilic activated carbon decorated nanopolymer foam for scalable, energy efficient photothermal steam generation, as an effective desalination system *Nanomaterials* **10** 2510

[29] Jiao L et al 2020 Recent advances in fiber-optic evanescent wave sensors for monitoring organic and inorganic pollutants in water *TrAC, Trends Anal. Chem.* **127** 115892
[30] Leung A et al 2006 Effects of geometry on transmission and sensing potential of tapered fiber sensors *Biosens. Bioelectron.* **21** 2202–9
[31] Pevec S and Donlagic D 2014 Miniature fiber-optic sensor for simultaneous measurement of pressure and refractive index *Opt. Lett.* **39** 6221–4
[32] Chen C H et al 2010 A multi-D-shaped optical fiber for refractive index sensing *Sensors (Basel, Switzerland)* **10** 4794–804
[33] South I 2010 Novel D-type fiber optic localized plasmon resonance sensor realized by femtosecond laser engraving *JLMN-Journal of Laser Micro/Nanoengineering* **5**
[34] Jiang L et al 2011 Femtosecond laser fabricated all-optical fiber sensors with ultrahigh refractive index sensitivity: modeling and experiment *Opt. Express* **19** 17591–8
[35] Pérez-Hernández J et al 2009 Mercury optical fibre probe based on a modified cladding of sensitised Al2O3 nano-particles *Sensors Actuators B* **143** 103–10
[36] Zhi-xue H, Song-yuan D and Kong-jia W 2002 Sensitizing mechanism and adsorption properties of dye-sensitized TiO2 thin films *Plasma Sci. Technol.* **4** 1475–80
[37] Irshad M S, Wang X, Abbas A, Yu F, Li J, Wang J, Mei T, Qian J, Wu S and Javed M Q 2021 Salt-resistant carbon dots modified solar steam system enhanced by chemical advection *Carbon N. Y* (https://doi.org/10.1016/j.carbon.2021.01.140)
[38] Nguyen T H, Sun T and Grattan K T 2019 A turn-on fluorescence-based fibre optic sensor for the detection of mercury *Sensors* **19** 2142
[39] Darroudi M et al 2020 Acenaphtoquinoxaline as a selective fluorescent sensor for Hg (II) detection: experimental and theoretical studies *Heliyon* **6** e04986
[40] Liu T et al 2019 Quantitative remote and on-site Hg2+ detection using the handheld smartphone based optical fiber fluorescence sensor (SOFFS) *Sensors Actuators B* **301** 127168
[41] Balasurya S et al 2020 Sensitive and robust colorimetric assay for the detection of Hg2+ at nanomolar level from real samples by TMPM functionalized Ag-Fe NCs and it's photocatalytic and antimicrobial activities *J. Environ. Chem. Eng.* **8** 104305
[42] Aydin Z, Wei Y and Guo M 2014 An 'off–on' optical sensor for mercury ion detection in aqueous solution and living cells *Inorg. Chem. Commun.* **50** 84–7
[43] Shukla G M et al 2019 Optimization of plasmonic U-Shaped optical fiber sensor for mercury ions detection using glucose capped silver nanoparticles *IEEE Sens. J.* **19** 3224–31
[44] De A et al 2020 Plasmonic sensing of Hg(II), Cr(III), and Pb(II) ions from aqueous solution by biogenic silver and gold nanoparticles *Inorganic and Nano-Metal Chemistry* 1–12
[45] Zhang Y-N et al 2018 Reflective mercury ion and temperature sensor based on a functionalized no-core fiber combined with a fiber Bragg grating *Sensors Actuators B* **272** 331–9
[46] Park J and Seo H 2020 Plastic optical fiber sensor based on in-fiber rectangular hole for mercury detection in water *Sensors Mater.* **32** 2117–25
[47] Martínez-Hernández M E, Goicoechea J and Arregui F J 2019 Hg2+ optical fiber sensor based on LSPR generated by gold nanoparticles embedded in LBL nano-assembled coatings *Sensors* **19** 4906
[48] Zhong X et al 2020 Hg2+ optical fiber sensor based on LSPR with PDDA-Templated AuNPs and CS/PAA bilayers *Applied Sciences* **10** 4845
[49] Tan S-Y et al 2018 Detection of mercury (II) ions in water by polyelectrolyte–gold nanoparticles coated long period fiber grating sensor *Opt. Commun.* **419** 18–24